Available online at www.sciencedirect.com
SCIENCE DIRECT®
International Journal of Mass Spectrometry 238 (2004) 47–53
International Journal of Mass Spectrometry
www.elsevier.com/locate/ijms

Threshold electron impact ionization studies of uracil

S. Denifl, B. Sonnweber, G. Hanel, P. Scheier, T.D. Märk*,[1]

Institut für Ionenphysik, Leopold Franzens Universität, Technikerstr. 25, A-6020 Innsbruck, Austria

Received 30 May 2004; accepted 26 July 2004
Available online 13 September 2004

Abstract

Electron impact ionization near the threshold of the DNA base uracil (U) was investigated using a high resolution hemispherical electron monochromator combined with a quadrupole mass spectrometer. The mass spectrum measured at the electron energy of 70 eV reveals a rich fragmentation pattern. For the parent ion and some of the most intense fragment ions we measured the ion efficiency curves near the threshold and determined the corresponding appearance energies (AEs) using a nonlinear least square fitting routine based on a Wannier type power law. The present AE(U^+/U)= 9.59 ± 0.08 eV is in good agreement with vertical ionization energies obtained in previous photoelectron spectroscopy experiments. The appearance energies for the two most abundant fragment ions are AE($C_3H_3NO^+$/U)= 10.89 ± 0.07 eV and AE(OCN^+/U)= 13.41 ± 0.10 eV.

Keywords: Threshold; Electron impact; Ionization; Uracil

1. Introduction

The uracil molecule ($C_4H_4N_2O_2$) (see Fig. 1 for the molecular structure) is one of the four bases in the ribonucleic acid (RNA). Like DNA, RNA is a macromolecule consisting of about 75 up to several 1000 nucleotides (the sugar-base-phosphate complex) which are linked by phosphodiesterbridges [1]. There are three major differences between RNA and DNA: (i) the sugar in RNA is ribose instead of deoxyribose, (ii) uracil replaces the DNA base thymine and, in addition, (iii) RNA consists only of one strand (except several RNA-viruses), i.e., RNA does not show the double helix structure of the DNA. RNA is the intermediate step between DNA and proteins because RNA is synthesized with instruction of the DNA and plays the key role for the protein synthesis. The other bases of both, RNA and DNA are adenine, cytosine and guanine.

The basic properties of isolated biomolecules like the ionization energy (IE) or the electron affinity (EA) are of fundamental interest for modeling processes like the interaction of radiation with the genome. In general radiation damage can be classified into the direct and indirect damage caused by the primary or secondary species. The primary high energy radiation (α, β, γ and ions) removes electrons from the molecular network along the radiation track which leads to subsequent charge transfer and energy dissipation processes. This leads to the rupture of bonds forming the secondary species like neutral or ionic radicals. The most abundant secondary species are electrons which are produced in excess of 4×10^4 electrons per 1 MeV energy deposited by the primary quantum [2]. These secondary electrons have initial kinetic energies up to 20 eV [3] before they are thermalized by inelastic collisions in 10^{-12} s. Damage to the genome is expected to be one third direct, i.e., energy from primary and secondary species is transferred directly into DNA and to the closely bound water molecules [4]. Two-third of the damage is indirect involving damage by radicals (like for example the highly reactive OH-radical) [5–7] which are formed in interaction of the radiation with water molecules and other biomolecules surrounding the DNA.

* Corresponding author. Tel.: +43 512 507 6240; fax: +43 512 507 2932.
E-mail address: tilmann.maerk@uibk.ac.at (T.D. Märk).
[1] Also adjunct professor at Department Plasma Physics, Comenius University, SK-84248 Bratislava, Slovak Republic.

1387-3806/$ – see front matter © 2004 Elsevier B.V. All rights reserved.
doi:10.1016/j.ijms.2004.07.010

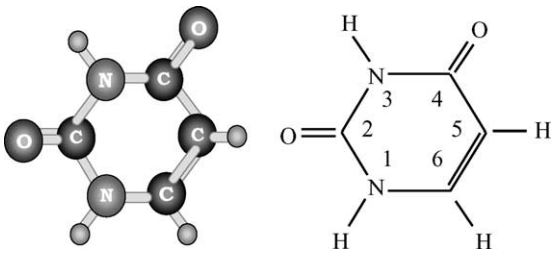

Fig. 1. Schematic drawing of uracil ($C_4H_4N_2O_2$) presented in a ball-stick model (left), where the small spheres represent the hydrogen atoms and the larger spheres represent the heavier atoms (labelled with atomic symbols) and a structure diagram of uracil (right).

Recent experiments have pointed out the importance of low energy secondary electrons which are able to induce single and double strand breaks of plasmid DNA also below the ionization threshold [8]. Similarities in the electron energy dependence of DNA strand breaks and negative ion desorption from thin films of biologically relevant molecules that were irradiated with an electron beam suggest that dissociative electron attachment is one of the processes that initiate strand breaks of DNA. Therefore, free electron attachment to isolated DNA/RNA components has been studied intensively and decomposition of these molecules was observed at electron energies as low as 1 eV [9–11]. In addition, the electron affinities of DNA/RNA bases have been determined in several experiments [12–15].

In this work we present electron impact ionization of neutral gas phase uracil. Starting from a mass spectrum taken at the electron energy of 70 eV we have measured ionization efficiency curves for the parent ion and the eight most intense fragment ions in order to determine the corresponding appearance energies (AEs). To the best of our knowledge, no previous experiments have been carried out to determine the AEs of fragment ions formed by electron impact of gas phase uracil. We intentionally use the expression "AE" and not ionization energy (IE) which is often found in literature. The IE is defined [16] as the lowest energy needed to remove an electron from a neutral molecule/atom in its ground state, whereas the expression AE is used for the threshold of fragment ions, i.e., simultaneous ionization and dissociation of the molecule. In the present study uracil molecules were evaporated in an oven and thus, the neutral molecules are vibrationally and rotationally excited. Therefore we define the expression AE as the minimum energy of the impacting electrons leading to the molecular ions observed (parent or fragment cation).

In a recent paper we compared a mass spectrum produced by electron impact of neutral uracil with the uracil mass spectrum produced by proton impact [17]. In addition we discussed in [17] briefly preliminary results for the AEs of the parent ion and the two most abundant fragment cations determined with the same apparatus that has been used for the present measurements. In the present report a detailed discussion of the results is given and, in addition, we present for the first time AEs of six additional fragment ions derived from measured ionization efficiency curves produced by electron impact of neutral gas phase uracil. For the parent cation of uracil the ionization energy via electron impact has been determined in three different previous studies [18–20]. All groups used the "method of Lossing" [21] for analyzing the measured ionization efficiency curves. Thereby the ionization efficiency curves of the studied cation and a calibration gas are normalized to the ion signal at a certain electron energy and logarithmically plotted as a function of the electron energy. Near the threshold a logarithmic ion yield exhibits a linear behavior which allows the determination of the ionization energy. The known value of the ionization energy of the calibration gas is used to define the energy scale.

In addition to electron impact ionization experiments eight UV-photoelectron spectroscopy measurements with uracil have been carried out [22–29]. All photoelectron spectra exhibit four electronic bands above the ionization energy starting from the lowest value of about 9.6 up to 11 eV. The first band (i.e., the lowest vertical IE) was assigned to the removal of the electron from the highest occupied π orbital (π_1). The IE of the second highest occupied orbital is at least 0.5 eV higher. Recently Wetmore et al. [30,31] calculated the vertical and adiabatic IEs and electron affinities EAs for nucleobases and for modified pyrimidines using ab initio methods and different levels of theory. Russo et al. [32] calculated the adiabatic IE and EA of uracil and other pyrimidines. All theoretical investigations showed that uracil exhibits the highest IE of all nucleobases

2. Experimental setup and data analysis

The present experiments were performed with a crossed molecule/electron beam instrument in combination with a quadrupole mass spectrometer (see Fig. 2). A detailed description of the experimental setup can be found in [33]. The electron beam is produced with a hair pin filament and has a typical energy spread of about 700 meV. This value

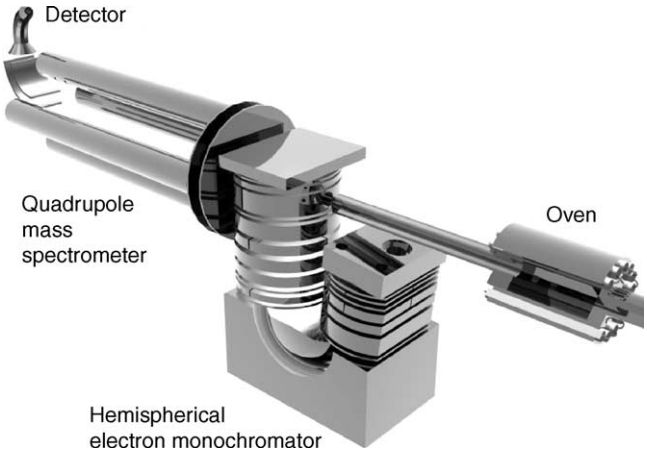

Fig. 2. Schematic view of the experimental setup.

can be reduced using a hemispherical electron monochromator down to a best value of 35 meV [34]. After the hemispheres the electron beam is accelerated to the desired energy and focused into the collision chamber where the interaction with the neutral molecule beam takes place. Finally the electron current is measured after the collision chamber at an electron collector plate. The electron current was recorded as a function of the electron energy. The ionization efficiency curves were normalized with the electron current in order to eliminate the influence of a changing electron current when scanning the electron energy. The maximum electron energy of the present experimental setup is 600 eV. For the present measurements the FHWM of the electron energy distribution was set to 100–150 meV for sufficiently high sensitivity of the apparatus. Uracil powder is vaporized in a Knudsen type oven and gas phase molecules are introduced directly into the collision chamber through an 8 cm long copper capillary with an opening at the end of 1 mm in diameter. The white powder of uracil was purchased from Sigma-Aldrich and has a purity of 99%. The vapor pressure of uracil was sufficiently high to form an intensive neutral molecular beam at the oven temperature of 180 °C (measured with a Pt100 temperature sensor attached directly on the oven). The cations formed by electron impact of the neutral uracil beam are extracted from the interaction region by a weak electrostatic field (at maximum 20 V/m) towards the entrance of a quadrupole mass spectrometer. The mass selected ions are detected by a channeltron type secondary electron multiplier (SEM). The pulses are processed using a pulse counting technique by a computer. The ionization efficiency curves for mass selected ions were measured by repeatedly ramping the electron energy over a pre-defined energy range including the threshold (generally several eV below the threshold up to about 5 eV above the appearance energy). The energy scale was calibrated shifting the measured appearance energy of Xe^+ or Kr^+ to the well known spectroscopic values [35] of 12.13 or 13.99 eV, respectively.

For the determination of the appearance energy of a certain cation we utilized a nonlinear least square fitting routine using the Marquart-Levenberg algorithm (for a detailed discussion see [36]). The measured ionization efficiency curve is fitted with the fit function $f(E)$ which resembles a Wannier threshold law (exponential type):

$$f(E) = b \quad \text{for } E < \mathrm{AE}_1 \tag{1a}$$

$$f(E) = b + c(E - \mathrm{AE}_1)^{p_1} \quad \text{for } \mathrm{AE}_1 < E < \mathrm{AE}_2 \tag{1b}$$

$$f(E) = b + c(E - \mathrm{AE}_1)^{p_1} + d(E - \mathrm{AE}_2)^{p_2} \quad \text{for } E > \mathrm{AE}_2 \tag{1c}$$

The fit for function (1b) comprises four parameters: a background signal b, a scaling constant c which is zero in (1a) (below the threshold), the appearance energy AE_1 and the exponent p_1 which is 1.127 for the ionized hydrogen atom according to the threshold law by Wannier [37]. In the case an ionization efficiency curve exhibits a second threshold due to an additional ionic state or a second process leading to an ion with the same mass per charge ratio function (1b) is extended with a third term leading to function (1c). AE_2 is then the corresponding AE of the second threshold. The fitting of the data was performed with the programs SIGMAPLOT or Origin. With this fitting method a reliable and reproducible determination of appearance energies can be achieved. This was demonstrated for rare gases and several simple molecules with nearly perfect agreement with the corresponding spectroscopic values [38]. Recently also electron impact ionization of more complex molecules [39–45] was studied using this analysis procedure.

3. Results and discussion

3.1. Mass spectrum

Fig. 3 shows the mass spectrum of uracil measured at the electron energy of 70 eV. The parent ion appears at mass 112 amu with the most abundance of all product cations. However, please note that both the quadrupole mass spectrometer and reduced ion collection efficiency of fragment ions that were formed with high initial kinetic energy may influence the relative abundance of the mass peaks. Uracil has this high abundance of the parent cation in common with other nucleobases [35]. In contrast, simple amino acids or sugar molecules appear to be more fragile. The most abundant fragment cations of uracil are $(C_3H_3NO)^+$ at mass 69 amu, $(OCN)^+$ (mass 42 amu) and $(CO)^+$ (mass 28 amu). A remarkable fact is that two nearly complementary product ions (except one hydrogen), i.e., $(OCN)^+$ and $(C_3H_3NO)^+$, appear in the mass spectrum with second and third highest in-

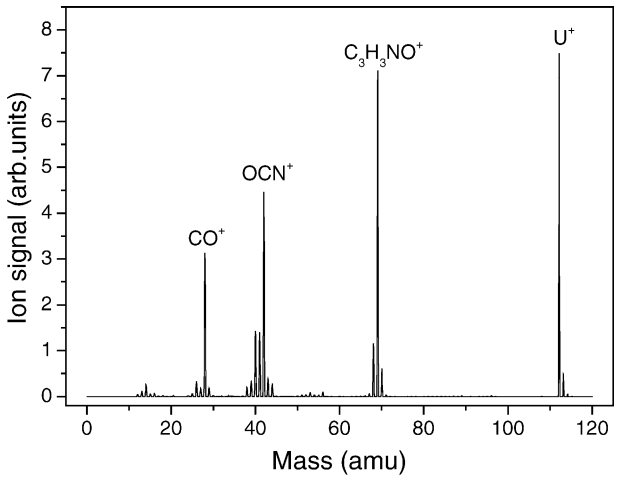

Fig. 3. Mass spectrum obtained by electron impact ionization of uracil at the electron energy of 70 eV.

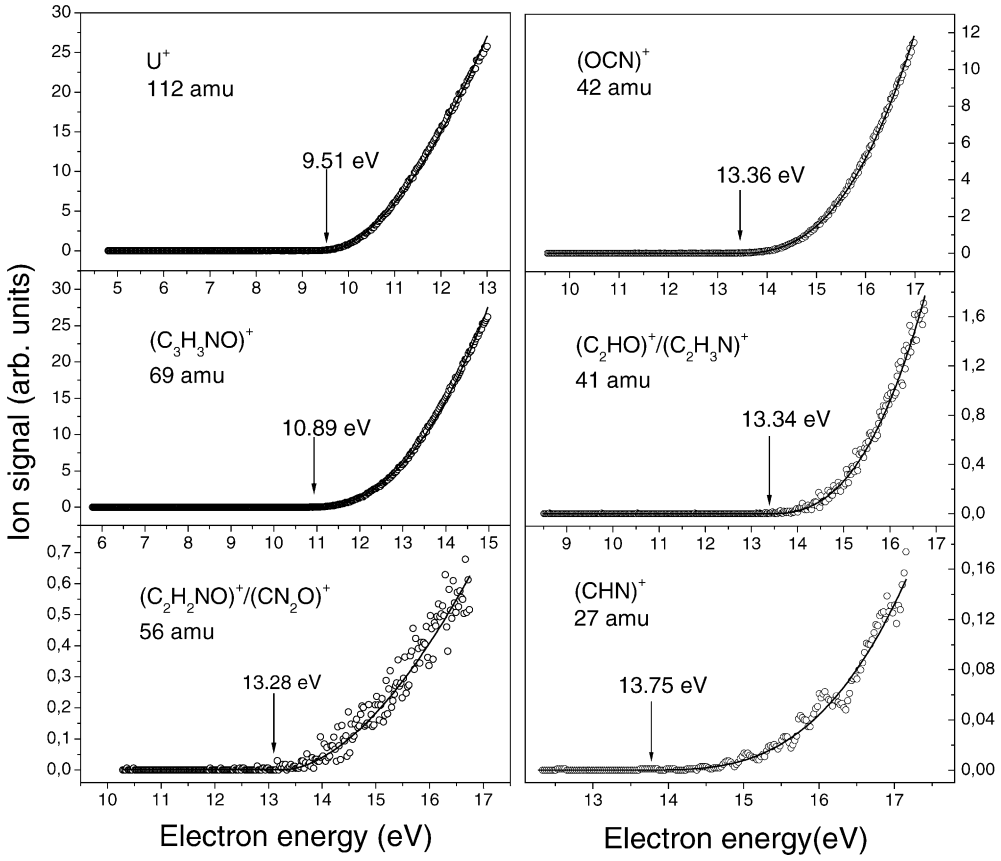

Fig. 4. Ionization efficiency curves near the threshold region for the formation of uracil cations from neutral uracil by electron impact. The measured data are shown as open circles whereas the fit curves (derived by the fitting procedure described in text) are shown as solid lines. The AEs indicated by arrows are the thresholds for these individual data sets and differ from the AEs given in the text and in Table 1 which were derived by averaging several values from individual data sets.

tensity. We cannot observe any dehydrogenated uracil cation (mass 111 amu). In contrast, $(U–H)^-$ is the most abundant anion formed by DEA to uracil [9]. In [17] a mass spectrum of uracil was already presented that was measured with the same instrument. Lower mass ions are much more abundant in the previously published mass spectrum [17]. The discrepancy to the presently obtained mass spectrum can be explained by (i) a higher electron energy of 200 eV in [17] and (ii) a different radiofrequency head of the quadrupole (0–512 amu) was used in [17] which has a higher transmission for low masses. We had to use this frequency head to resolve the H^+ ion formed by electron impact of neutral uracil (this product ion was formed with high intensity by proton impact ionization of uracil). The hydrogen cation is not included in the present mass spectrum as it was measured with a frequency head that has a mass range from 2 to 2048 amu.

The NIST database contains a mass spectrum of uracil measured by electron impact ionization at an electron energy of 70 eV [35]. There is good agreement between this mass spectrum and the present one. The peaks at mass 18 and 17 amu are much higher in the NIST mass spectrum compared to the present data, thus indicating a lower water content of the presently used sample.

3.2. Appearance energies

For the parent ion and eight fragment cations we measured the ionization efficiency curves near the threshold and determined the corresponding appearance energies (AEs) using the fit procedure described above. Fig. 4 shows the ion efficiency curves (open circles) and the corresponding fits (solid lines) for the parent cation and five fragment ions. In Table 1 the AEs of all ions investigated are listed. The present AE values in this table were derived by averaging the results of

Table 1
AE for cations of uracil produced by electron impact on neutral uracil

Cation produced by electron impact of uracil	Mass (amu)	Present AE value (eV)
U^+	112	9.59 ± 0.08
$(C_3H_3NO)^+$	69	10.89 ± 0.07
$(C_3H_2NO)^+$	68	12.75 ± 0.66
$(C_2H_2NO)^+/(CN_2O)^+$	56	13.20 ± 0.25
$(OCNH)^+$	43	13.36 ± 0.30
$(OCN)^+$	42	13.41 ± 0.10
$(C_2HO)^+/(C_2H_3N)^+$	41	13.32 ± 0.18
$(CH_2N)^+/(CO)^+$	28	13.83 ± 0.39
$(CHN)^+$	27	14.77 ± 0.92

The values are the mean values of several individual data sets.

several data sets and the uncertainties were calculated as the difference between the largest and smallest values of the AEs derived from the different measurements. In contrast the values in Fig. 4 are the individual result for the data set shown.

The parent ion has an AEs value of 9.59 ± 0.08 eV which represents the lowest AE value of all cations investigated in this work. The most abundant fragment ion appearing at mass 69 amu $(C_3H_3NO)^+$ has a threshold value of 10.89 ± 0.07 eV. We also determined the AE of the fragment ion one amu below, i.e., involving the additional removal of a hydrogen atom from the molecule. This leads to an increase by 1.9 eV to an AE of 12.75 ± 0.66 eV. We also determined the AE of the fragment cation at mass 56 amu which can be ascribed to the formation of $(C_2H_2NO)^+$ or $(CN_2O)^+$, respectively. The latter cations appear at the half of the mass of the intact uracil molecule. Moreover, we measured the ionization efficiency curves at masses 41–43 amu where the most abundant cation is $(OCN)^+$ at mass 42 amu. The ions in this mass region and the cation at mass 56 amu have very similar AEs near 13.3 eV. Nevertheless we can exclude that the measured ionization efficiency curve at mass 43 amu is only resulting from the isotope yield of $(OCN)^+$ with the ^{13}C isotope. The calculated abundance of the isotope on mass 43 amu is 1.5% of the intensity on mass 42 amu. In the present mass spectrum the peak height at mass 43 is 8.5% of the intensity of mass 42 amu indicating indeed the formation of $(OCNH)^+$. The AE value of $(CH_2N)^+/(CO)^+$ at mass 28 amu is approximately 0.5 eV higher than for the cations near mass 42 amu. In contrast to the cations in the mass region from 41–43 amu the additional removal of one hydrogen from the $(CH_2N)^+$ complex leading to $(CHN)^+$ gives an AE value which is nearly 1 eV higher than that for $(CH_2N)^+/(CO)^+$.

Table 2 includes for comparison all previous experimentally and theoretically determined values of the vertical ionization energy of uracil. As mentioned above, the IE for electron impact ionization of uracil has been measured already by three different groups. Lifshitz et al. [18] obtained the value of 9.82 ± 0.1 eV which is 230 meV larger than the present value (9.59 ± 0.08 eV), whereas lower values were given by the other two studies (Verkin et al. [19]: 9.35 ± 0.1 eV; Zaretskii et al. [20]: 9.53 ± 0.02 eV). The previous investigations of the IE of uracil by electron impact can be expected to be less accurate (with an error of at least ±0.3 eV [46]) because the electron energy resolution in these experiments was much worse (≥0.5 eV) than in the present study using an electron monochromator.

Table 2
Comparison of the present AE value for the parent cation of uracil with previous determinations of the vertical ionization energy of uracil

U^+/Uracil		
Author	Method	AE (in eV)
Present	EI	9.59 ± 0.08
Lifshitz et al. [18]	EI	9.82 ± 0.1
Verkin et al. [19]	EI	9.35 ± 0.1
Zaretskii et al. [20]	EI	9.53 ± 0.02
Padva et al. [22]	PE	9.59 ± 0.02
Hush et al. [23]	PE	9.50 ± 0.03
Dougherty et al. [24]	PE	9.60/9.34[a]
Lauer et al. [25]	PE	9.45
Palmer et al. [26]	PE	9.68
Yu et al. [27]	PE	9.59 ± 0.03
Urano et al. [28]	PE	9.59
Kubota and Kobayazhi [29]	PE	9.53 ± 0.01
Wetmore et al. [30,31]	Theory	9.47/9.21[a]
Russo et al. [32]	Theory	9.25[a]

The previous methods are electron impact (EI), UV photoelectron spectroscopy (PE) and theoretical calculations, respectively.
[a] Adiabatic IE value.

The calculated value by Wetmore et al. [31] of 9.47 eV for the vertical ionization of uracil is 120 meV lower than the present value. A similar difference was observed for thymine where a recent experimental value [47] for the AE of thymine is 130 meV higher than the calculated one. In general good agreement exists between the present value and vertical ionization energies determined in UV photoelectron spectroscopy. The values range from 9.45 to 9.68 eV [22–29] with appropriate uncertainties of 0.02–0.03 eV [46]. Nevertheless the lowest value of 9.45 eV by Lauer et al. [25] seems to be questionable due to an obvious calibration error [46] indicated by a general discrepancy in their IEs of all bands in comparison to other works. The present value is in perfect agreement with results of [22,24,27,28] within the error of 10 meV. Values for the adiabatic ionization energy (AIE) are also included in Table 3. Theoretical values of the AIE were calculated by Russo et al. [32] (9.25 eV) at the B3LYP/6-311++G** level of theory and Wetmore et al. [30] (9.21 eV) at the B3LYP/6-31+G(2df, p) level of theory. Older semi empirical theoretical works using the AM1 method which has less accuracy than the ab initio calculations, resulted in a value for the AIE of uracil of 9.20 eV [48] (not included in Table 2). The values for the AIE are significantly lower than the value for the vertical IE. Thus uracil exhibits in this connection a similar behavior as many other molecules, such as C_6H_6 [42], C_3H_8 [39] and OClO [49], indicating a direct ionization mechanism in the electron impact event. Nevertheless recent electron impact ionizations experiments [50] exhibit threshold values for diatomic molecules which have been very close to the adiabatic value. Such results may be explained by an indirect ionization mechanism via the excitation of a Rydberg state with subsequent associative ionization within the molecule [40].

In comparison with the AEs of the parent ions of 5-Chlorouracil (5-ClU) and 6-Chlorouracil (6-ClU) [51], which belong to the class of halouracils, the presently determined value of the AE of the parent ion of uracil is remarkably similar. The AE of 5-ClU^+/5-ClU (9.38 ± 0.05 eV) turns out to be 0.21 eV lower whereas for 6-ClU^+/6-ClU (9.71 ± 0.05 eV) the AE value is 0.12 eV higher compared to the AE of U^+/U. For comparison the AE values for the parent ion and the two most abundant fragment cations formed via electron impact ionization of the three different molecules are shown in Fig. 5. A similar trend of the AE values is obtained for uracil and 5-ClU. However, the AEs cannot be compared directly

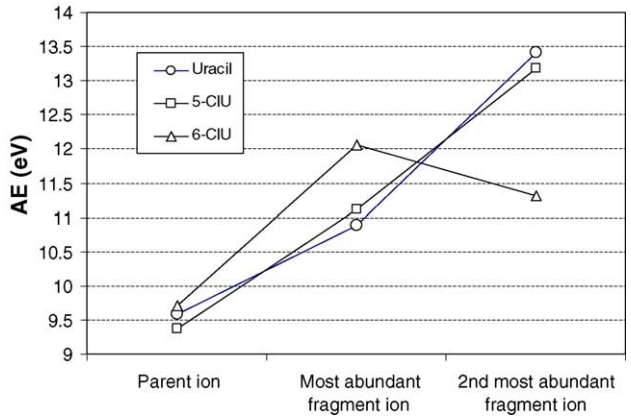

Fig. 5. Comparison of the AEs for the parent cation and the two most abundant fragment ions of uracil (circles), 5-ClU (squares) and 6-ClU (triangles) formed by electron impact of neutral uracil, 5-ClU and 6-ClU. The similarity between the three systems seems to disagree with the fact that halouracils incorporated in DNA act as radiosensitizers (see text).

because the fragment cations with most abundance have different composition. It is interesting to note that at an electron energy of 70 eV the mass spectrum of uracil exhibits the strongest fragmentation of all three molecules. These unexpected results have important consequences for the investigation of the underlying mechanism of radiosensitizers because according to the present results, the increased sensitivity of cells modified with halouracils cannot be explained by enhanced fragmentation of the cations. However, in contrast to positive ion formation much stronger differences in the properties of uracil and halouracils can be found in negative ion formation where low energy electrons form fragment anions and neutral radicals via dissociative electron attachment to neutral 5-ClU and 6-ClU with much higher efficiency than in the case of uracil [52].

Acknowledgment

This work has been supported by the FWF, and ÖNB, Wien, Austria and the European Commission, Brussels.

References

[1] L. Stryer, Biochemistry, 1st edition, W.H. and Company, San Francisco, 1975.
[2] International Commission on Radiation Units and Measurements. ICRU Report 31. Washington, DC: ICRU, 1979.
[3] V. Cobut, Y. Fongillo, J.P. Patau, T. Goulet, M.-J. Fraser, J.-P. Jay-Gerin, Radiat. Phys. Chem. 51 (1998) 229.
[4] B.D. Michael, P.A. O'Neill, Science 287 (2000) 1603.
[5] M. Folkard, K.M. Prise, B. Brocklehurst, B.D. Michael, J. Phys. B: At. Mol. Opt. Phys. 32 (1999) 2753.
[6] C.M. DeLara, T.J. Jenner, K.M.S. Townsend, S.J. Marsden, P. O'Neill, Radiat. Res. 144 (1995) 43.
[7] J.K. Wolken, E.A. Syrstad, S. Vivekananda, F. Turicek, J. Am. Chem. Soc. 123 (2001) 5804.
[8] B. Boudaiffa, P. Cloutier, D. Hunting, M.A. Huels, L. Sanche, Science 287 (2000) 1658.
[9] S. Denifl, S. Ptasińska, M. Cingel, S. Matejcik, P. Scheier, T.D. Märk, Chem. Phys. Lett. 377 (2003) 74.
[10] R. Abouaf, J. Pommier, H. Dunet, Int. J. Mass. Spectr. 226 (2003) 397.
[11] H. Abdoul-Carime, S. Gohlke, E. Illenberger, Phys. Rev. Lett. 92 (2004) 168103.
[12] J. Schiedt, R. Weinkauf, D.M. Neumark, E.W. Schlag, Chem. Phys. 239 (1998) 511.
[13] J.H. Hendricks, S.A. Lyapustina, H.L. de Clercq, J.T. Snodgrass, K.H. Bowen, J. Chem. Phys. 104 (1996) 7792.
[14] C. Desfrancois, H. Abdoul-Carime, J.P. Schermann, J. Chem. Phys. 104 (1996) 7792.
[15] K. Aflatooni, G.A. Gallup, P.D. Burrow, J. Phys. Chem. 102 (1998) 6205.
[16] F.H. Field, J.L. Franklin, Electron Impact Phenomena, Academic Press, New York, 1957.
[17] B. Coupier, B. Farizon, M. Farizon, M.J. Gaillard, F. Gobet, N.V. de Castro Faria, et al., Eur. Phys. J. D 20 (2002) 459.
[18] C. Lifshitz, E.D. Bergmann, B. Pullmann, Tetrahedron Lett. 46 (1967) 4583.
[19] B.I. Verkin, L.F. Sukodub, I.K. Yanson, Dokl. Akad. Nauk. SSSR 228 (1976) 1452.
[20] V.I. Zaretskii, V.L. Sadovskaya, N.S. Wulfson, V.F. Sizoy, V.G. Merimson, Org. Mass. Spectrom. 5 (1971) 1179.
[21] F.P. Lossing, A.W. Tickner, W.A. Bryce, J. Phys. Chem. 19 (1951) 1254.
[22] A. Padva, P.R. LeBreton, R.J. Dinerstein, J.N.A. Ridyard, Biochem. Biophys. Res. Commun. 60 (1974) 1262.
[23] N.S. Hush, A.S. Cheung, Chem. Phys. Lett. 34 (1975) 11.
[24] D. Dougherty, K. Wittel, J. Meeks, S.P. McGlynn, J. Am. Chem. Soc. 98 (1976) 3815.
[25] G. Lauer, W. Schafer, A. Schweig, Tetrahedron Lett. 45 (1975) 3939.
[26] M.H. Palmer, I. Simpson, R.J. Platenkamp, J. Mol. Struct. 66 (1980) 243.
[27] C. Yu, T.J. O'Donnell, P.R. LeBreton, J. Phys. Chem. 85 (1981) 3851.
[28] S. Urano, X. Yang, P.R. LeBreton, J. Mol. Struct. 214 (1989) 315.
[29] M. Kubota, T. Kobayashi, J. El. Spectros. Rel. Phen. 82 (1996) 61.
[30] S.D. Wetmore, R.J. Boyd, L.A. Eriksson, Chem. Phys. Lett. 322 (2000) 129.
[31] S.D. Wetmore, R.J. Boyd, L.A. Eriksson, Chem. Phys. Lett. 343 (2001) 151.
[32] N. Russo, M. Toscano, A. Grand, J. Comput. Chem. 21 (2000) 1243.
[33] D. Muigg, G. Denifl, A. Stamatovic, T.D. Märk, Chem. Phys. 239 (1998) 409.
[34] G. Denifl, D. Muigg, I.C. Walker, P. Cicman, S. Matejcik, J.D. Skalny, et al., Czech. J. Phys. 49 (1999) 383.
[35] NIST chemistry web book, http://webook.nist.gov.
[36] S. Matt, O. Echt, R. Wörgötter, V. Grill, P. Scheier, C. Liftshitz, et al., Chem. Phys. Lett. 264 (1997) 149.
[37] G.H. Wannier, Phys. Rev. 90 (1953) 817.
[38] G. Hanel, T. Fiegele, A. Stamatovic, T.D. Märk, Zeitschrift für Physikalische Chemie 214 (2000) 1137.
[39] T. Fiegele, G. Hanel, I. Torres, M. Lezius, T.D. Märk, J. Phys. B: At. Mol. Opt. Phys. 33 (2000) 4263.
[40] G. Hanel, J. Fedor, B. Gstir, M. Probst, P. Scheier, T.D. Märk, J. Phys. B: At. Mol. Opt. Phys. 35 (2002) 589.
[41] B. Gstir, G. Hanel, M. Probst, P. Scheier, N.J. Mason, T.D. Märk, J. Phys. B: At. Mol. Opt. Phys. 35 (2002) 1567.
[42] G. Hanel, B. Gstir, T. Fiegele, F. Hagelberg, K. Becker, P. Scheier, et al., J. Chem. Phys. 116 (2002) 2456.
[43] A. Abedi, P. Cicman, B. Coupier, B. Gulejova, P. Scheier, T.D. Märk, Int. J. Mass. Spectrom. 232 (2004) 147.
[44] P. Cicman, K. Gluch, A. Pelc, W. Sailer, S. Matt-Leubner, P. Scheier, et al., J. Chem. Phys. 119 (2003) 11704.

[45] S. Ptasińska, S. Denifl, P. Scheier, T.D. Märk, J. Chem. Phys. 120 (2004) 8505.
[46] T.J. O'Donnell, P.R. LeBreton, J.D. Petke, L.L. Shipmann, J. Chem. Phys. 84 (1980) 1975.
[47] S.K. Kim, W. Lee, D.R. Herschbach, J. Phys. Chem. 100 (1996) 7933.
[48] Q. Zhang, E.C.M. Chen, Biochem. Biophys. Res. Comm. 246 (1995) 755.
[49] M. Probst, K. Hermansson, J. Urban, P. Mach, D. Muigg, G. Denifl, et al., J. Chem. Phys. 116 (2002) 984.
[50] D.L. Hildebrand, Int. J. Mass Spectrom. Ion Proc. 197 (2000) 237.
[51] S. Denifl, S. Ptasińska, B. Gstir, P. Scheier, T.D. Märk, Int. J. Mass Spectrom. 232 (2004) 99.
[52] S. Denifl, S. Matejcik, S. Ptasińska, B. Gstir, M. Probst, P. Scheier, et al., J. Chem. Phys. 120 (2004) 704.